NOTES AND CORRESPONDENCE

Assessing the Vertical Distribution of Convective Available Potential Energy

DAVID O. BLANCHARD

NOAA/National Severe Storms Laboratory, Boulder, Colorado

13 January 1998 and 25 March 1998

ABSTRACT

Comparisons of convective available potential energy (CAPE) with standard instability indices for evaluating the convective potential of the atmosphere such as the lifted index (LI) reveal only moderate correlations. This is because the LI is a measure of single-level buoyancy while CAPE is a measure of both integration depth and the buoyancy. Normalizing the CAPE values by the depth over which the integration takes place provides an index (NCAPE) that is independent of the depth and is a convenient measure of the mean parcel buoyancy. This normalization effectively distinguishes between environments with similar CAPE but exhibiting different buoyancy and integration depth. Also, because the vertical distribution of CAPE can have an important effect on convective updraft strength, it is advantageous to vertically partition CAPE and NCAPE into multiple layers. NCAPE may provide a more useful indicator of buoyancy in environments in which the depth of free convection is shallow and total CAPE is small. It is suggested that NCAPE computations be used in combination with CAPE for evaluation of convective potential.

1. Introduction

The use of single-valued indices to evaluate the state of the atmosphere is a time-honored tradition and one that continues as new indices are continually introduced and evaluated. Many of these indices are designed specifically to evaluate the convective and severe weather potential of the atmosphere and may combine measures of the thermal and moisture properties, and the wind shear of the low and midtroposphere. These indices include the Showalter index (SI; Showalter 1953), lifted index (LI; Galway 1956), total–totals (Miller 1967), total energy index (Darkow 1968), severe weather threat (Miller et al. 1971), convective available potential energy (CAPE; Moncrieff and Miller 1976), bulk Richardson number (Weisman and Klemp 1982), energy–helicity index (Hart and Korotky 1991), vorticity generation potential (Rasmussen 1998, manuscript submitted to *Wea. Forecasting*), and many others. An excellent description of many atmospheric indices is given by Peppler (1988).

Each of these indices has strengths and weaknesses, and no single index can be thought to provide a complete characterization of the state of the atmosphere. In fact, important details of the lapse rate structure may be smoothed out or completely missed in these indices. For example, the SI is defined as the difference between the ambient temperature at 500 mb and the 500-mb temperature that a parcel will achieve if it is lifted dry adiabatically from 850 mb to its condensation level and then moist adiabatically to 500 mb. This index can lead to unrepresentative values if the moisture does not extend upward from the surface to 850 mb, or if the surface is elevated and results in an inadequate representation of the boundary layer. The SI becomes undefined when the surface pressure is less than 850 mb. Additionally, the SI is a ''static index'' based on the temperature and dewpoint at the time of the sounding and does not take into account changes that may occur as afternoon heating occurs.

The LI is computed in a manner similar to that of the SI except for the determination of the lifted parcel pressure, temperature, and dewpoint. The parcel is assigned the mean mixing ratio of the lowest 1000 m (common variations typically use the lowest 500 m, 50 mb, or 100 mb) and the potential temperature corresponding to the dry adiabat passing through a predicted afternoon maximum temperature. The LI, then, is a ''forecast index'' because it attempts to use anticipated conditions. The LI, as well as the SI, is susceptible to unrepresentative values of instability if the temperature at 500 mb is unrepresentative of the environment above or below, such as might occur if a midtropospheric inversion or stable layer is present. The SI is rarely used nowadays,

* Additional affiliation: Cooperative Institute for Mesoscale Meteorological Studies, University of Oklahoma, Norman, Oklahoma.

Corresponding author address: David O. Blanchard, NOAA/NSSL 325 Broadway, Boulder, CO 80303.
E-mail: blanch@ucar.edu

but the LI remains in regular use in both operational and research work.

In recent years, the use of CAPE has become very popular as a method to evaluate the convective potential of the atmosphere. In contrast to single-level stability indices, CAPE is a vertically integrated index and measures the cumulative buoyant energy in the free convective layer (FCL) from the level of free convection (LFC; the level at which the parcel temperature exceeds the ambient temperature and parcels are unstable relative to their environment) to the equilibrium level (EL; the level at which the ambient temperature exceeds the parcel temperature and parcels are stable relative to their environment). The formal definition is given by

$$\text{CAPE} = g \int_{z_{\text{LFC}}}^{z_{\text{EL}}} \left(\frac{T_{v_p} - T_{v_e}}{T_{v_e}} \right) dz, \qquad (1)$$

where T_{v_p} is the virtual temperature of the parcel and T_{v_e} is the virtual temperature of the environment, Z_{EL} is the height of the equilibrium level, Z_{LFC} is the level of free convection, and g is gravity. This definition of CAPE uses the method described by the United States Air Force (USAF) Air Weather Service (AWS 1961) and more recently by Doswell and Rasmussen (1994) in which temperature is replaced by virtual temperature. The computed value of CAPE can vary significantly depending on the choice of parcel used. Doswell and Rasmussen discuss some of the different methods available for the determination of the initial parcel.

As the cumulative experience in both the operational and research environment grows, certain behavioral characteristics of CAPE have become apparent and need to be fully understood to take advantage of the information contained within this index.

2. Interpretation of CAPE

Measures of the positive area on a sounding diagram have been given different names over the years. The USAF Air Weather Service (which changed its name to the Air Force Weather Agency in 1997) simply called it positive area (AWS 1961). Moncrieff and Miller (1976) were the first to use the term convective available potential energy. Fritsch and Chappell (1980) called it potential buoyant energy (PBE). Variations of this include +BE and net positive buoyant energy. Despite the abundance of names, it now appears that CAPE is the de facto standard terminology. AWS defined the integral in (1) using virtual temperature; Moncrieff and Miller (1976) and Fritsch and Chappell (1980) used temperature.

It should be pointed out that CAPE is not a measure of instability (Moncreiff and Miller 1976), at least in the same sense as the LI or SI in which a temperature excess between the parcel and the environment at a single level is evaluated. The appropriate units of the LI and SI are degrees. CAPE is, rather, a vertically integrated measure of the parcel buoyant energy with appropriate units of joules per kilogram. Similarly, Fritsch and Chappell (1980) note that the positive area is the buoyant energy that would accrue to a parcel in rising between its LFC and EL. Nonetheless, it has often been used as a proxy for instability and as a substitute for the LI for many years, and, as a result, its usage needs to be evaluated in that context.

a. Aspect ratio of the positive area

If one views a ''true'' thermodynamic diagram (i.e., one on which area is proportional to energy) such as the skew T–log$p$ diagram or the tephigram, it is apparent that the positive area [i.e., the integral in (1), and the area between the ambient temperature profile and the moist adiabat of the lifted parcel] is constrained by two parameters: 1) the depth of the FCL from the LFC to the EL, and 2) the average magnitude of buoyancy, characterized by the virtual temperature excess ΔT_v, between lifted parcel and environment. If one can fix the value of CAPE (i.e., the positive area) and increase (decrease) the depth of the FCL, then the average magnitude of the buoyancy must decrease (increase) throughout the FCL. Thus, it is appropriate to consider the aspect ratio of the positive area (i.e., whether the CAPE is ''tall and thin'' or ''short and wide'') when one interprets CAPE values.

Recent work by Lucas et al. (1994a,b) poses the question of why oceanic convection has weaker vertical velocities than continental convection for environments with equivalent CAPE. They note that over the ocean the positive area on the sounding is generally ''skinny'' with small instability, but is maintained through a large fraction of the troposphere. In continental regions, the positive area is described as ''fat'' with large instability but over a shallower depth of the troposphere. They conclude that the continental sounding has a larger virtual temperature excess that may be significant when considering the effects of water loading on updraft velocity. Zipser and LeMone (1980) noted similar findings in their analysis of oceanic convection and claim that CAPE may be an overly simplistic measure of convective instability. Similar findings concerning the relationship of positive area to instability were noted in AWS (1961).

Clearly, soundings with similar CAPE but different aspect ratios can exhibit a large range of instability as computed by the more simplistic LI. Thus, it should now be apparent that there is not a one-to-one relationship between the integrated buoyant energy of CAPE and the temperature excess of the LI and other similar indices. This issue is discussed in more detail in section 3.

b. Buoyancy and vertical velocity

Recent modeling work by Wicker and Cantrell (1996) examining ''mini-supercells'' (Kennedy et al. 1993; Da-

vies 1993) presented interesting results concerning the role of low-level CAPE. Mini-supercells are defined as convective storms with low tops (generally below 6–8 km) and small horizontal scales for both the storm and mesoscyclone. They used three soundings having different CAPE values of 600, 1100, and 2200 J kg^{-1}. The temperature and moisture profiles for all three soundings were identical below 500 mb, and so the vertical profile of positive buoyancy was the same below this level. Their results show that the coupling of low-level shear and low-level CAPE (i.e., CAPE confined to or present only in the lowest few kilometers) appeared to be more important to the development of rotational characteristics within the storm than did the larger values of CAPE available through a deeper FCL. For example, the time-averaged vertical velocity profiles of Wicker and Cantrell (1996) show similar velocities up through about 5 km for all three environments, suggesting that the evaluation of low-level CAPE is appropriate to the determination of accelerations and vertical velocities in these lower levels.

Additional modeling work by McCaul and Weisman (1996) lends support to the idea that the distribution of CAPE is important. Using vertical profiles with the same CAPE (800 J kg^{-1}), they modified the thermal profiles so that the maximum buoyancy occurred at different vertical levels. For their zero-wind simulations, they found the peak evanescent updraft for the case with buoyancy maximized at 2.75 km had vertical velocities of ~35 m s^{-1}, almost double the 19 m s^{-1} value for the case where the buoyancy was maximized at 5.82 km.

Also, Johns and Doswell (1992) and Moller et al. (1994) noted that a substantial fraction of supercells nationwide arise in situations with CAPE less than 1500 J kg^{-1}. It is possible that many of these may have occurred in environments with small total CAPE but relatively large values of low-level CAPE. The results of these modeling and observational studies strongly suggest that the vertical distribution of CAPE, and especially low-level CAPE, can play a significant role in the development and evolution of convective storms and that it may be desirable to partition the total CAPE into CAPE for multiple layers.

3. Methodology of computation technique

This section presents some simple, yet informative, methods for evaluating the vertical distribution and magnitude of buoyancy associated with the CAPE and convective inhibition (CIN; Colby 1984).

a. Normalized CAPE and CIN

As discussed in section 2, it is appropriate to examine the aspect ratio of CAPE, or positive area, on a sounding. Presented here is a simple method of quantifying the aspect ratio. The normalized CAPE (NCAPE) is defined as the total CAPE divided by the depth of the FCL, that is,

$$\text{NCAPE} = \text{CAPE/FCL}, \tag{2}$$

where FCL $= Z_{\text{EL}} - Z_{\text{LFC}}$. NCAPE has units of joules per kilogram per meter, which simplifies to meters per second squared (i.e., an acceleration). Since CAPE has been scaled by its depth, it now represents the average buoyancy, or acceleration, for the depth of the FCL. Because NCAPE is an acceleration, it is now clear why the aspect ratio of the total CAPE is an important feature when assessing the growth potential of convective clouds, as noted by Zipser and LeMone (1980) and Lucas et al. (1994a,b).

Alternatively, CAPE can be scaled by the depth of the FCL in millibars (i.e., FCL $= P_{\text{LFC}} - P_{\text{EL}}$). The units, then, are joules per kilogram per millibar. Although the pressure-scaled version does not express its results as a simple acceleration, it is preferable because the units are a normalized form of the familiar units of CAPE. Experience with the pressure-scaled ratio indicates that values typically fall in the range of 1–6 J kg^{-1} mb^{-1}.

CIN is a measure of the ''negative area'' on the sounding diagram and the amount of work required to lift a parcel through a layer that is warmer than the parcel and allow these parcels to ascend above the LFC.[1] This negative area is often referred to as a lid. CIN is computed in a manner similar to CAPE and is defined as

$$\text{CIN} = g \int_{z_{\text{SFC}}}^{z_{\text{LFC}}} \left(\frac{T_{v_p} - T_{v_e}}{T_{v_e}} \right) dz, \tag{3}$$

where Z_{SFC} is the height of the surface and Z_{LFC} is the height of the LFC. One can also produce an aspect ratio index by scaling the CIN by the depth of the negative area; that is,

$$\text{NCIN} = \text{CIN}/(Z_{\text{LFC}} - Z_{\text{SFC}}), \tag{4}$$

where NCIN is the normalized CIN. CIN, like CAPE, can have varying aspect ratios. A given value of CIN can be distributed over a deep layer such that the magnitude of convective stability ΔT_v, or lid, is small at any

[1] The AWS manual (AWS 1961) defines two types of negative areas. In the case of surface-parcel heating, the negative area lies in the area from the surface up to the convective condensation level. This is the negative area that must be overcome by surface heating. This negative area will appear on the warm side of the environmental temperature curve on a thermodynamic diagram and is bounded by the dry adiabat corresponding to the convective temperature. In the case of lifted surface parcels, the negative area lies between the lifting condensation level and the LFC. This is the negative area that must be overcome when lifting occurs from some mechanical process (e.g., orographic, frontal, or convergence) and convective temperature has not been achieved. This negative area will appear on the cool side of the environmental temperature curve on a thermodynamic diagram and is bounded by the moist adiabat of the ascending parcel.

particular level; conversely, the vertical depth for a given value of CIN may be very shallow and ΔT_v will be large at any level.

b. Vertical partitioning of CAPE

As mentioned in section 2 it is desirable to partition the total CAPE into CAPE for different layers. Recent modeling results (Wicker and Cantrell 1996; McCaul and Weisman 1996) suggest that (relatively) large values of low-level CAPE and the associated strong accelerations just above cloud base may be critically important to the development of low-level pressure perturbations and low-level mesocyclones. In an operational environment it is important to have a quick and easy method to describe the vertical distribution of total CAPE and low-level CAPE. Computing CAPE from the LFC to a level that is, say, 3 km above the LFC (LFC3) is simple and can quickly indicate how much buoyant energy is available in the region just above the cloud base. This is accomplished simply by modifying the limits of integration:

$$\mathrm{CAPE}_{\mathrm{LFC3}} = g \int_{z_{\mathrm{LFC}}}^{z_{\mathrm{LFC3}}} \left(\frac{T_{v_p} - T_{v_e}}{T_{v_e}} \right) dz. \qquad (5)$$

Further, one can compute the normalized low-level CAPE; that is,

$$\mathrm{NCAPE}_{\mathrm{LFC3}} = \mathrm{CAPE}_{\mathrm{LFC3}}/(Z_{\mathrm{LFC3}} - Z_{\mathrm{LFC}}). \qquad (6)$$

It should be noted that the selection of a layer that is 3 km deep is arbitrary; one could as easily select a different layer or even multiple layers.

4. Examples

Some examples of CAPE, LI, and NCAPE are presented in this section to help visualize the features discussed in the previous section. Comparisons are made between soundings with similar CAPE but different NCAPE to illustrate how variations in the depth of the FCL can change CAPE.

Rawinsonde data were selected to be representative of varying airmass environments typically experienced during the warm season over the United States. Dodge City, Kansas (DDC), Tampa Bay, Florida (TBW), and Greensboro, North Carolina (GSO), were selected as representative of the high plains environment, subtropical environment, and modified subtropical/middle-latitude environment, respectively. Soundings were retrieved from the *Radiosonde Data of North America 1946–1995 CD-ROM* distributed by the NOAA Forecast Systems Laboratory and NOAA National Climatic Data Center.

All 1200 UTC soundings for these stations were retrieved for the warm season (i.e., March–August) for the 5-yr period 1990–94. Morning soundings from 1200 UTC were used because they were less likely to be convectively contaminated than, say, the 0000 UTC soundings. Each sounding was processed, and soundings with positive values of CAPE were selected for further review, resulting in 595 soundings from DDC, 791 from TBW, and 460 from GSO.

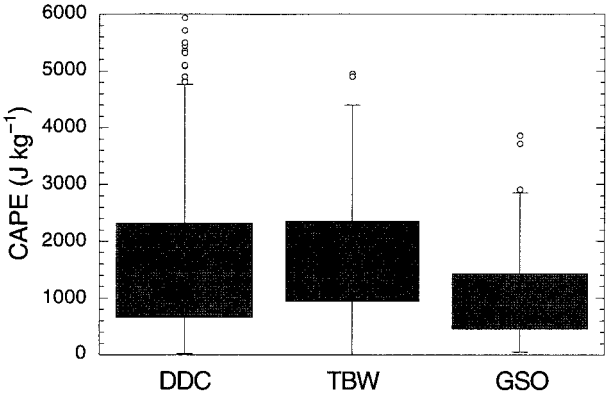

FIG. 1. Box plot showing distribution of CAPE for the three sounding sites at DDC, TBW, and GSO. The shaded box encloses 50% of the data, with the median value of the variable displayed as a horizontal line. The top and bottom of the box mark the limits of ±25% of the variable population. The lines extending from the top and bottom of each box mark the minimum and maximum values that fall within an acceptable range. The acceptable range is defined as UQ + 1.5 (IQD) or LQ − 1.5 (IQD), where UQ (LQ) is the upper (lower) quartile and IQD is the interquartile distance (UQ − LQ); outliers are used in the calculations of the box plot. Any value outside this range is displayed as an individual point.

CAPE and LI were computed as follows: First, the mean mixing ratio ($\overline{w}$) in the lowest 500 m was computed. (This depth may be too shallow for DDC where the boundary layer can occasionally grow deeper than 500 m. For purposes of comparison, the same depth was used for all three stations.) From this value, the convective condensation level (CCL) and convective temperature (T_c) were determined. Parcels were assumed to have attained T_c with moisture $\overline{w}$. These parcels were lifted dry adiabatically to the CCL, then moist adiabatically to the equilibrium level. With this approach, there was no surface-based negative area, or CIN, left to overcome although there certainly could be CIN elevated above the CCL level. This method probably represents an upper limit of CAPE for a given sounding. Both CAPE and LI were computed using the virtual temperature (AWS 1961; Doswell and Rasmussen 1994) for consistency, even though the LI traditionally uses temperature.

In Fig. 1, the distributions of CAPE are compared for three locations (DDC, TBW, and GSO) using a box plot. The shaded box encloses 50% of the data, with the median value of the variable displayed as a horizontal line. The top and bottom of the box mark the limits of ±25% of the variable population. The vertical lines extending from the top and bottom of each box mark the minimum and maximum values that fall within an acceptable range. Any value outside this range, called an outlier, is displayed as an individual point. It can be

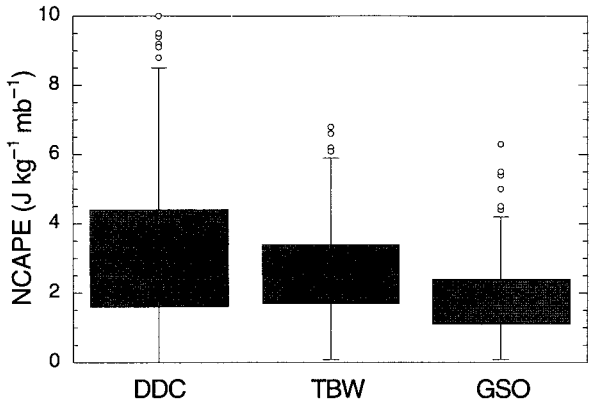

FIG. 2. As in Fig. 1 except for the distribution of NCAPE for the three sounding sites at DDC, TBW, and GSO.

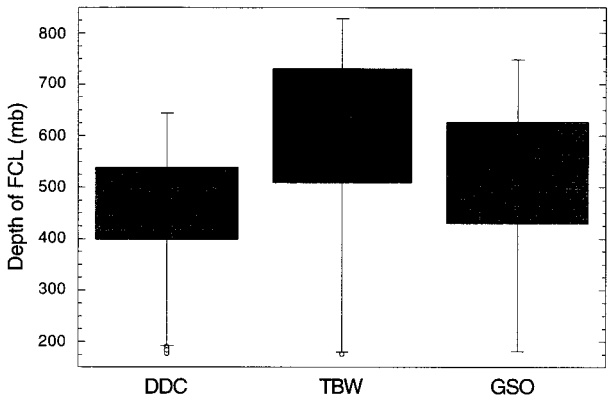

FIG. 3. As in Fig. 1 except for the distribution of the depth of the FCL for the three sounding sites at DDC, TBW, and GSO.

seen that the general distribution of CAPE values for DDC and TBW is similar, although the range of values is greater for DDC than TBW, while the median for DDC (~1415 J kg^{-1}) is less than that of TBW (1740 J kg^{-1}). The median value for GSO is 905 J kg^{-1} and shows a smaller range of values than either DDC or TBW.

Figures 2 and 3 help to put these values into perspective. Figure 2 shows the distribution of NCAPE for DDC, TBW, and GSO. What is immediately evident is that DDC and TBW have similar median values (2.9 vs 2.6 J kg^{-1} mb^{-1}). On the other hand, the distribution of the interquartile distance (IQD; i.e., the central 50% of values) is very different, and indicates that TBW has a limited IQD of NCAPE that falls in the range 1.7–3.4 J kg^{-1} mb^{-1}. IQD values of NCAPE for DDC range from 1.6 to 4.4 J kg^{-1} mb^{-1}. GSO shows the smallest range of values for NCAPE (1.1–2.4 J kg^{-1} mb^{-1}) as well as the lowest median value (1.6 J kg^{-1} mb^{-1}).

Figure 3 shows the distribution of the depth of the FCL for the DDC, TBW, and GSO soundings. The box plot clearly shows that there are significant differences in the FCL for these three sites, with DDC showing the shallowest depth and TBW the deepest. This result illustrates that the depth of the FCL, one of the two components that define CAPE, exhibits considerable variability. It is to be expected, then, that CAPE shows variability that is related, in part, to the FCL depth rather than virtual temperature excess ΔT_v. Examination of the effects of topography, LFC, and tropopause heights (not shown) indicated that the primary factor in the variation in FCL is attributable to the LFC variations, and secondarily to the tropopause (and EL) heights. Effects of topography are tertiary.

Figure 4 is a scattergram of CAPE versus LI for DDC, TBW, and GSO. The CAPE values have been limited to the range of 1000–3000 J kg^{-1} so that a few extreme values at the high end of CAPE and the large cluster of values near the low end do not excessively influence the statistics. (The lower threshold is arbitrary but changing it to, say, 750 J kg^{-1} does not appreciably change the results.) In this range, coefficients of determination, R^2 (correlation coefficients, R), between CAPE and LI for DDC, TBW, and GSO are 0.44 (0.66), 0.56 (0.75), and 0.55 (0.74), respectively. Here, R^2 can be interpreted as the fraction of the total variation that is explained by the least squares regression line, suggesting that for all three sites almost 50% of the variation in CAPE is due to causes other than instability (i.e., ΔT_v). These results clearly indicate that there is only a moderate correlation between CAPE (integrated parcel buoyancy) and LI (single-level virtual temperature excess) and that variations in CAPE must be the result of both the instability *and* the depth of the FCL. Not surprisingly, examination of Fig. 4 shows that for a CAPE value of 2000 J kg^{-1}, one can get an LI ranging from roughly −3.5 to −7.5, a rather large range of LI values.

Figure 5 is a scattergram of CAPE versus depth of the FCL for DDC, TBW, and GSO. All three sites show a marked increase in the depth of the FCL for increasing CAPE up to ~1000 J kg^{-1}. Note that even as CAPE

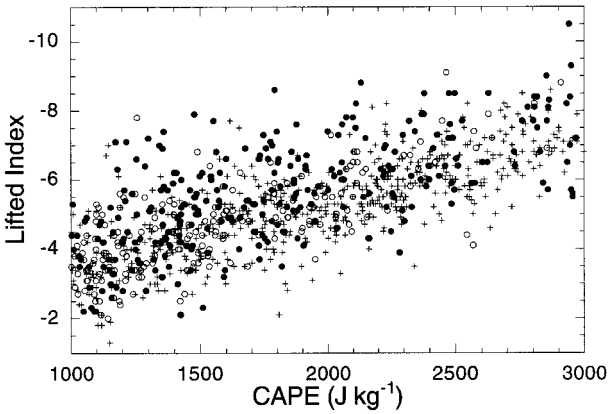

FIG. 4. Scattergram of CAPE versus LI for DDC (filled circles), TBW (pluses), and GSO (open circles). The range of CAPE has been limited to fall between 1000 and 3000 J kg^{-1}.

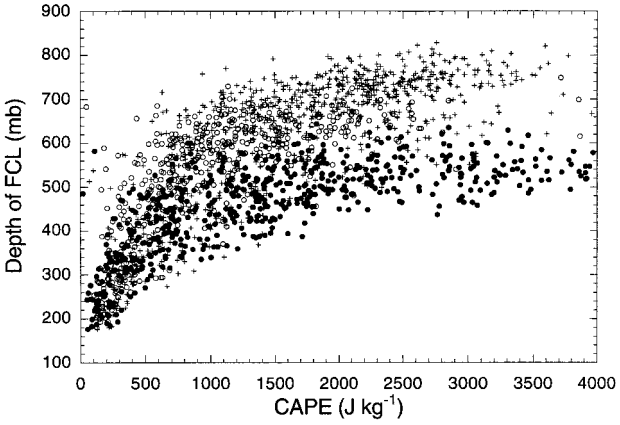

FIG. 5. Scattergram plot of CAPE versus depth of the FCL for DDC (filled circles), TBW (plus), and GSO (open circles).

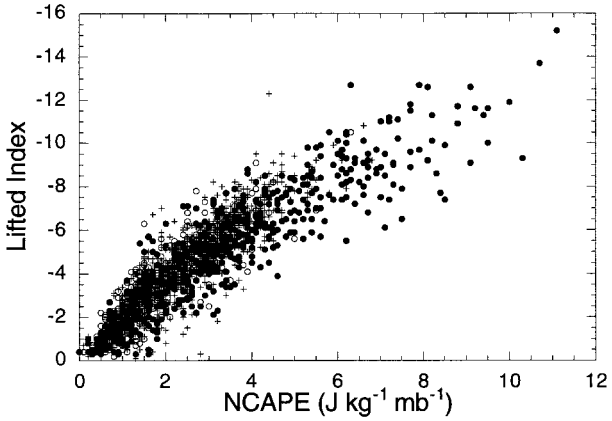

FIG. 6. Scattergram of NCAPE versus LI for DDC (filled circles), TBW (pluses), and GSO (open circles).

increases beyond ~1500 J kg^{-1} in the TBW and GSO soundings, the depth of the FCL continues to show a corresponding increase. On the other hand, as CAPE increases beyond about 1500 J kg^{-1} at DDC, only small increases in the depth of the FCL are noted. This suggests that, to a first approximation, increases of CAPE at GSO and TBW can be primarily attributed to increases in the depth of the FCL and secondarily to increases in buoyancy. Increases in CAPE above ~1500 J kg^{-1} for DDC show a decreasing rate in the growth in the depth of the FCL, suggesting that increases in CAPE at this site can be primarily attributed to increases in buoyancy and secondarily to increases in the depth of the FCL. Note, also, that for a given value of CAPE the depth of the FCL is larger at GSO and TBW than at DDC, indicating that DDC typically has greater buoyancy than TBW or GSO for a given value of CAPE.

Figure 6 is a scattergram of NCAPE versus LI for DDC, TBW, and GSO. The correlation coefficients R (coefficients of determination R^2) between NCAPE and LI for DDC, TBW, and GSO are 0.91 (0.83), 0.88 (0.77), and 0.87 (0.76), respectively. These are notably higher values than for the comparison between CAPE and LI indicate that NCAPE may be a better indicator of mean buoyancy than CAPE is. In fact, computation of NCAPE for the mini-supercell sounding presented by Davies (1993) gives 1.8 J kg^{-1} mb^{-1} for a sounding with only 915 J kg^{-1} total CAPE. This value falls into either the second (DDC, TBW) or third (GSO) quartile of NCAPE distributions and clearly indicates that this sounding had significant instability despite small total CAPE.

Finally, comparison is made between two skew T–log$p$ diagrams (Figs. 7 and 8). Both soundings have similar CAPE (DDC: 2293 J kg^{-1}; TBW: 2286 J kg^{-1}) but are otherwise quite different in their buoyancy characteristics. Figure 7 shows the sounding at DDC. The temperature and moisture profile for DDC suggest an environment that may not achieve convective temperature during the day, or one in which the low-level moisture may ''mix out'' resulting in an environment in which convection might not occur; for purposes of the example, these issues have been ignored. Figure 8 shows the sounding at TBW. Although values of CAPE differ by less than 1%, the LFC (EL) for TBW is considerably lower (higher) than for DDC. The result is that the depth of the FCL is significantly larger for TBW than for DDC. Examination of the LI shows that there is greater instability at DDC (−6.7 °C) than TBW (−5.5 °C). Similarly, the NCAPE values reveal that there is greater buoyancy at DDC (4.9 J kg^{-1} mb^{-1}) than at TBW (3.0 J kg^{-1} mb^{-1}). Examination of the low-level CAPE ($CAPE_{LFC3}$) also indicates significant differences. DDC has $CAPE_{LFC3}$ of 541 J kg^{-1}. TBW, on the other hand, has $CAPE_{LFC3}$ of 335 J kg^{-1}. This difference suggests

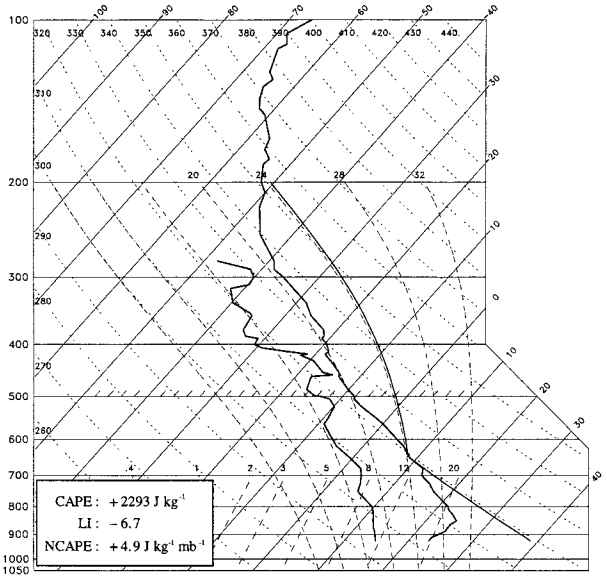

FIG. 7. Skew T–log$p$ diagram for DDC. Heavy, solid lines are (left to right) the dewpoint, dry-bulb temperature, and adiabat of parcel ascent. CAPE, LI, and NCAPE values are given. Calculations of CAPE, NCAPE, and LI are based on virtual temperature of the environment and virtual temperature of the ascent adiabat.

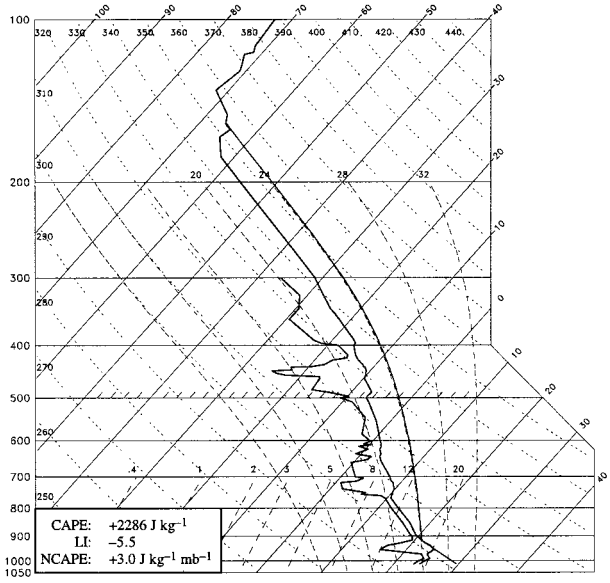

FIG. 8. As in Fig. 7 except for TBW.

that the accelerations and vertical velocities in this layer will be greater for the DDC sounding than for the TBW sounding.

These examples clearly demonstrate the points made in the previous sections. CAPE does not always provide a good measure of buoyancy because it is a result of both depth of the FCL and the buoyancy. Only when the total CAPE is scaled by the depth of the free convective layer can we obtain a measure of the (layer mean) buoyancy and discriminate between soundings with large versus small aspect ratio of CAPE

5. Summary

In recent years, the use of convective available potential energy (CAPE) has become very popular as a method to evaluate the convective potential of the atmosphere. As the cumulative experience using CAPE grows, certain behavioral characteristics have become apparent and need to be fully understood to take advantage of the information contained within this index.

CAPE is not a simple measure of instability (i.e., a temperature excess between parcel and environment); rather, it is a vertically integrated measure of the parcel buoyant energy. Comparisons of CAPE with standard instability indices such as the lifted index reveal only moderate correlations. The correlation coefficients R (coefficients of determination R^2) between CAPE and LI for DDC, TBW, and GSO are 0.66 (0.44), 0.75 (0.56), and 0.74 (0.55), respectively. The low correlations indicate that these two indices are measuring different characteristics of the environment.

Because CAPE is an integration of parcel buoyancy from the level of free convection to the equilibrium level, it follows that CAPE is sensitive to both the magnitude of buoyancy and the depth of the integration. Environments may have similar CAPE but different degrees of instability if one environment is characterized by tall and thin CAPE and the other by short and wide CAPE. The results presented here concur with the statements made by Zipser and LeMone (1980) that CAPE may be an overly simplistic measure of instability.

To account for the variations in CAPE that can be attributed to differences in the depth of the free convective layer, the CAPE is normalized by the depth over which the integration takes place. This normalized CAPE provides an index that is a better measure of instability. The correlation coefficient R (coefficient of determination R^2) between NCAPE and LI for DDC, TBW, and GSO are 0.91 (0.83), 0.88 (0.77), and 0.87 (0.76), respectively. Scaling CAPE by the depth in height provides an NCAPE with units of meters per second squared, an acceleration. This simple result clarifies why determining the aspect ratio of buoyancy to depth for the CAPE index is advantageous. Simple parcel theory states that the vertical velocity attained by a buoyant parcel at the EL is dependent only on the total CAPE. Accelerations, however, are strongly dependent on the aspect ratio of the CAPE and the buoyancy distribution. Parcels will experience greater accelerations when large values of CAPE are a result of large buoyancy rather than great depth between the LFC and EL. Further, simple parcel theory neglects the effects of water loading, entrainment and detrainment, and pressure perturbations. As noted by Lucas et al. (1994a,b) a larger virtual temperature excess may be significant when considering the effects of water loading on updraft velocity.

Recent work on mini-supercells have shown that these environments typically have low values of CAPE. Yet the NCAPE for these environments is similar to that in the more classical severe weather environments. This result shows that NCAPE can provide a better indicator of buoyancy in environments in which the depth of free convection is shallow.

It is also important to note that some geographical areas of the United States (e.g., the western high plains) will always have a more shallow depth of the FCL because of a larger mixed boundary layer and higher convective condensation levels. In these regions, the limited depth of the FCL generally means that increases in CAPE can be primarily attributed to increases in buoyancy. In other regions, increases in CAPE can be attributed both to increases in buoyancy and to the depth of the FCL. Thus, direct comparisons of CAPE between regions with shallow FCLs and regions with deep FCLs should be made with caution.

Finally it is not suggested that we abandon the use of CAPE in the evaluation of convective potential. Instead, users should continue to compute CAPE and add the computation of NCAPE to their toolbox. Evaluating NCAPE can quickly point out whether the CAPE is a product primarily of buoyancy or of the depth of the FCL. Alternatively, the user could evaluate the mean

LI over many levels and the depth of the FCL, or CAPE and FCL, or other possible combinations. The underlying issue here is to consider both some integrated or mean measure of parcel temperature excess and the depth of the FCL.

Future work on the importance of NCAPE and the vertical partitioning of CAPE should include a climatology of NCAPE and storm types (e.g., ordinary, supercell, tornadic) to ascertain whether these tools assist in discriminating between storm types. This work should also examine the possibility that regional variations in the distribution of NCAPE appear to explain regional differences in ''typical'' storm types better than do regional variations in the distribution of total CAPE.

Acknowledgments. The author thanks Professor Frederick Sanders for discussions in 1991 in which the ideas of aspect ratios of CAPE and CIN were discussed in regard to convective initiation and inhibition. The work presented here is a direct consequence of the ideas presented at those meetings. An appreciative thanks is extended to Dr. Robert Maddox for providing thoughtful commentary on an early draft of the manuscript. Thanks are also extended to my many colleagues for their suggestions for improving the text and to Jon Davies for providing sounding data. This work was supported in part by National Science Foundation Grant ATM-9617318.

REFERENCES

AWS, 1961: Use of the skew *T*-log*p* diagram in analysis and forecasting. Vol. 1. AWSM 105–124, 144 pp. [Available from Headquarters, Air Force Weather Agency, Scott AFB, IL 62225.]

Colby, F. P., Jr., 1984: Convective inhibition as a predictor of convection during AVE-SESAME II. *Mon. Wea. Rev.,* **112,** 2239–2252.

Darkow, G. L., 1968: The total energy environment of severe storms. *J. Appl. Meteor.,* **7,** 199–205.

Davies, J. M., 1993: Small tornadic supercells in the central plains. Preprints, *17th Conf. on Severe Local Storms,* St. Louis, MO, Amer. Meteor. Soc., 305–309.

Doswell, C. A., III, and E. N. Rasmussen, 1994: The effect of neglecting the virtual temperature correction on CAPE calculations. *Wea. Forecasting,* **9,** 625–629.

Fritsch, J. M., and C. F. Chappell, 1980: Numerical prediction of convectively driven mesoscale pressure systems. Part I: Convective parameterization. *J. Atmos. Sci.,* **37,** 1722–1733.

Galway, J. G., 1956: The lifted index as a predictor of latent instability. *Bull. Amer. Meteor. Soc.,* **37,** 528–529.

Hart, J. A., and W. Korotky, 1991: The SHARP workstation version 1.5, A skew-t/Hodograph Analysis and Research Program for the IBM and compatible PC, NOAA Eastern Reg. Comput. Programs, 58 pp. [Available from National Weather Service, Bohemia, NY 11716.]

Johns, R. H., and C. A. Doswell III, 1992: Severe local storms forecasting. *Wea. Forecasting,* **7,** 588–612.

Kennedy, P. C., N. E. Westcott, and R. W. Scott, 1993: Single-Doppler radar observations of a mini-supercell tornadic thunderstorm. *Mon. Wea. Rev.,* **121,** 1860–1870.

Lucas, C., E. J. Zipser, and M. A. LeMone, 1994a: Vertical velocity in oceanic convection off tropical Australia. *J. Atmos. Sci.,* **51,** 3182–3193.

——, ——, and —— 1994b: Convective available potential energy in the environment of oceanic and continental clouds: Corrections and comments. *J. Atmos. Sci.,* **51,** 3829–3930.

McCaul, E. W., and M. L. Weisman, 1996: The dependence of simulated storm structure on variations in the shapes of environment buoyancy and shear profiles. Preprints, *18th Conf. on Severe Local Storms,* San Francisco, CA, Amer. Meteor. Soc., 718–722.

Miller, R. C., 1967: Notes on analysis and severe storm forecasting procedures of the Military Weather Warning Center. AWS Tech. Rep. 200 (revised), 170 pp. [Available from Headquarters, Air Force Weather Agency, Scott AFB, IL 62225.]

——, A. Bidner, and R. A. Maddox, 1971: The use of computer products in severe weather forecasting (the SWEAT index). Preprints, *Seventh Conf. on Severe Local Storms,* Kansas City, KS, Amer. Meteor. Soc., 1–6.

Moller, A. R., C. A. Doswell III, M. P. Foster, and G. R. Woodall, 1994: The operational recognition of supercell thunderstorm environments and storm structures. *Wea. Forecasting,* **9,** 327–347.

Moncrieff, M. W., and M. J. Miller, 1976: The dynamics and simulation of tropical cumulonimbus and squall lines. *Quart. J. Roy. Meteor. Soc.,* **102,** 373–394.

Peppler, R. A., 1988: A review of static stability indices and related thermodynamic parameters. Illinois State Water Survey Misc. Publ. 104, 87 pp. [Available from Illinois State Water Survey, Champaign, IL 61820.]

Rasmussen, E. N., 1998: A baseline climatology of sounding-derived supercell and tornado forecast parameters. *Wea. Forecasting,* in press.

Showalter, A. K., 1953: A stability index for thunderstorm forecasting. *Bull. Amer. Meteor. Soc.,* **34,** 250–252.

Weisman, M. L., and J. B. Klemp, 1982: The dependence of numerically simulated convective storms on vertical wind shear and buoyancy. *Mon. Wea. Rev.,* **110,** 504–520.

Wicker, L. J., and L. Cantrell, 1996: The role of vertical buoyancy distributions in miniature supercells. Preprints, *18th Conf. on Severe Local Storms,* San Francisco, CA, Amer. Meteor. Soc., 225–229.

Zipser, E. J., and M. A. LeMone, 1980: Cumulonimbus vertical velocity events in GATE. Part II: Synthesis and model core structure. *J. Atmos. Sci.,* **37,** 2458–2469.